Indian Journal of Science and Technology, *Vol 7(12), 2020–2032, December 2014*
ISSN (Print) : 0974-6846
ISSN (Online) : 0974-5645

CFD Analysis of Aortic Aneurysms on the Basis of Mathematical Simulation

H. Girija Bai[1], K. B. Naidu[2] and G. Vasanth Kumar[3]

[1]Research Scholar, Sathyabama University, Chennai-600 119, Tamil Nadu, India; girijanameprakash@gmail.com
[2]Department of Mathematics, Sathyabama University, Chennai-600 119, Tamil Nadu, India; kbnaidu999@gmail.com
[3]Department of Aeronautical Engineering, Sathyabama University, Chennai-600 119, Tamil Nadu, India; vassa.aero@gmail.com

Abstract

In the present study, Aortic Aneurysms (AA) are investigated using Computational Fluid Dynamics (CFD) softwares Fluent and Gambit. A computational model of AA is developed from computed tomography (CT) scans using MIMICS software. Hemodynamic factors such as velocity magnitude, dynamic pressure, wall shear stress, wall strain, streamline patterns for unsteady flow conditions are discussed in detail. Contours and streamline patterns show how the flow is affected by different input pressure (p = 90.0074 mmHg, 150.0123 mmHg, 180.0148mmHg) and velocity (v = –0.4 m/s, –0.6 m/s, –1.5 m/s) conditions. The interruption of blood flow is visible through high pressure and low velocities in the region of aneurysms. These techniques based on computer flow study are important for understanding the relationship between hemodynamic parameters and risk of rupture. Quantification and decision of multiple aneurysms serve as the root for surgical intervention.

Keywords: Aortic Aneurysms, Computational Fluid Dynamics, Contours, Hemodynamic, Mimics, Streamlines

1. Introduction

In developed countries the majority of deaths are caused by cardiovascular diseases, most of which are connected with some form of irregular blood flow in arteries. The arteries are living organs that can adjust and change with the varying hemodynamic conditions. Hemodynamics refers to physiological factors governing the flow of blood in the circulatory system. An aneurysm is a balloon-like dilation found on the walls of a blood vessel or a sac formed by the localized dilatation of the wall of an artery or a vein, or the heart. Unprocessed aneurysm may rupture under insistent internal pressure, causing a fatality or severe disability. Even an unruptured aneurysm can lead to damage by interrupting the flow of blood or by impinging on the wall of the vessel, in some cases eroding nearby blood vessel, organs, or bone. Aneurysms are seen most often in large arteries such as the iliac, femoral, popliteal, carotid or renal arteries. There are different types of aneurysms according to their sizes such as small, medium, large and giant. Similarly, depending on their shape; 1. Saccular (sac-like) with a well-defined neck 2. Saccular with wide neck 3. Fusiform (spindle shaped) without a distinct neck. The aorta is the large artery that carries oxygen-rich blood from the heart to various parts of our body. This artery extends from the heart down through the chest and abdominal region, where it divides into blood vessels that supply to each leg. An aneurysm can develop anywhere in arteries. If it occurs in the aorta, we term as aortic aneurysm (AA- an abnormal bulge in the wall of the aorta). Aneurysm occurs in the abdominal aorta (Abdominal Aneurysms) and in the section that runs through our chest (Thoracic Aneurysms). An aortic aneurysm is serious because - depending on its size - it may rupture, causing life-threatening internal bleeding. The risk of an aneurysm rupturing increase as the

**Author for correspondence*

aneurysm gets larger. The risk of rupture also depends on the location of the aneurysm. Each year, approximately 15,000 Americans die of a ruptured aortic aneurysm. When detected in time, an aortic aneurysm can usually be repaired with surgery.

Several numerical studies[1–7] have been carried out recently to trace the hemodynamic factors in the blood vessels. Analysis of unsteady flow dynamics is very important in understanding the influence of arterial diseases in vessels and in the design of artificial organs. Blood flow has been numerically analyzed by Wille[8] in moderately dilated rigid blood vessels to trace streamlines of the flow. Similarly, the pathlines of the flow particles were analyzed[9–11]. Taylor and Yamaguchi[12] have carried out numerical studies on 2D/3D models of aneurysms. Liang-Der Jou; Michel E Mawad[13] have analyzed the growth rate and rupture rate of unruptured intracranial aneurysms. David Roy et al.[14] were reviewed on the numerical analysis of abdominal aortic aneurysms. The simulation of complex dynamic processes that appear in nature or in industrial applications poses a lot of challenging mathematical problems, opening a long road from the basic problem, to the mathematical modeling, the numerical simulation, and finally to the interpretation of results.

Viscous, incompressible, unsteady blood flow conditions under various blood pressure and velocities were taken into the present study. Analysis shows how the blood flow is affected by aortic aneurysms for different input conditions. Our study shows the contours of velocity, pressure, wall shear stress, wall strain and patterns of streamlines in the computational model. Limitations on the amount of the dilations are ignored. Since arterial wall is gently elastic, we neglect the wall dispensability. Change in diameter in arteries is on the order of 10% McDonald, D. A.[15] so error in fixed diameter is small.

2. Methodology

In the field of medical research, several computational tools are being developed to help biomedical researchers and clinicians in the investigation of aneurysm initiation, growing, and risk of rupture. Without a visualization of these complex data, it is not possible to understand the correlations between specific hemodynamic characteristics and their influence on the development of the aneurysm. MIMICS and Computational fluid dynamics (CFD) are used in many areas, such as medical field and engineering. This new field provides very detailed information about fluid characteristics. Medical science lent this new technology to study hemodynamic within the body. CFD uses Finite Volume Method (FVM) such as FDM. In FVM, two interpolation structures can be used: (i) Piecewise constant interpolation (ii) Piecewise linear (or bilinear) interpolation. First is denoted by cell-centered method and the second are denoted by the cell-vertex method. In both methods, the cells and group of cells around a node are used as volumes. In the present study MIMICS and CFD software are used for image processing and for numerical simulations. The 809 compressed CT images Figure 1a. of 0.8398 pixels in the DICOM form of Volume: 2039530.59 mm3, Surface: 1262911.09 mm2, Triangles: 2864398, Points: 1446919 is loaded with MIMICS software. By using segmentation techniques such as thresholding, region growing and cropping the image was reduced in volume: 102286.38 mm3, surface: 29152.05 mm2, triangle: 47628, points: 23690 (Figure 2d). Different views of the cropped image such as Sagital, Coronal, Axial and 3D are shown in Figure 2a, Figure 2b, Figure 2c, and Figure 2d. 3D view clearly shows the aneurysms in two parts of the aorta. The data were taken from MIMICS and imported to CFD software Gambit. The mesh is generated in Gambit; using pave mesh of size 0.5 is shown in Figure 3a and export of CFD software FLUENT v.6.3.26 (ANSYS. Inc.) where the domain is processed in 3 stages, namely pre-processing, processing and post processing. Governing equations were solved in FLUENT which use a finite volume method. The solutions of hemodynamic factors such as velocity, pressure, shear stress, strain shows the growth and rupture of aneurysms.

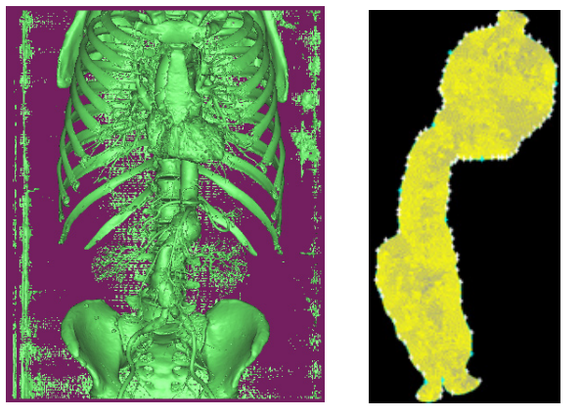

Figure 1. Real and Model of Aortic Aneurysms for analysis.

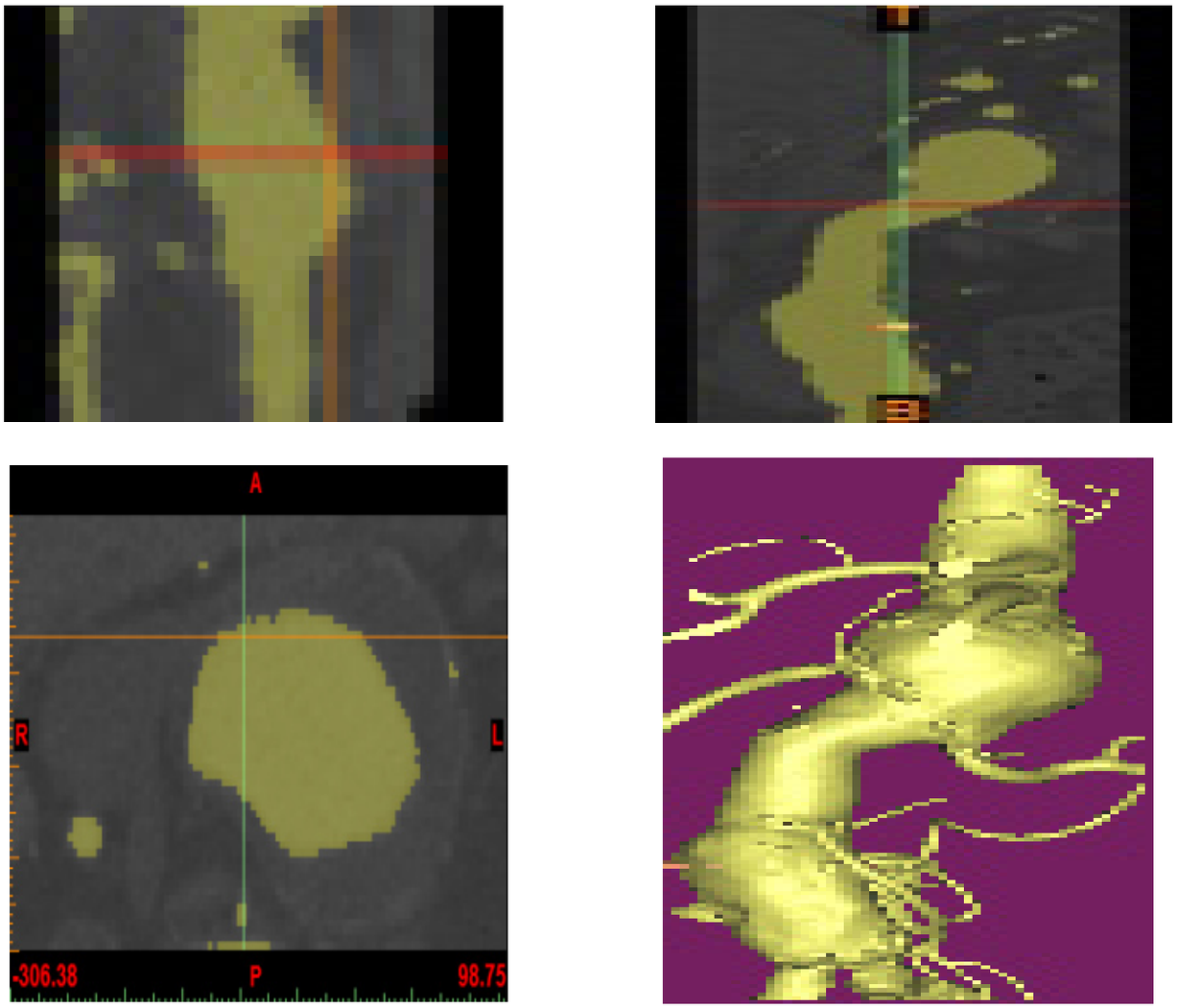

Figure 2. Sagital, Coronal, Axial and Three dimensional view of Aortic Aneurysms.

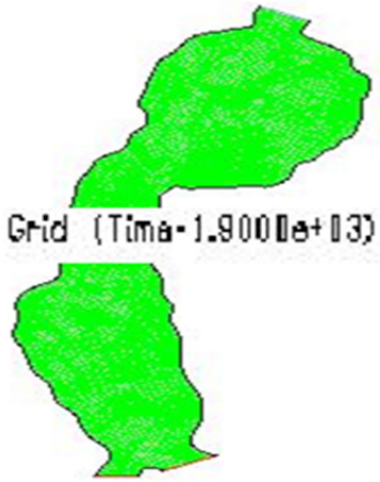

Figure 3. Pave mesh of size 0.01.

3. Description of Mathematical Model

In the present study, dynamic model of virtual aortic aneurysms has taken into consideration. The governing partial differential equations are unsteady Navier-Stokes equations:

$$\nabla \cdot \vec{v} = 0 \tag{1}$$

$$\rho\left(\frac{\partial \vec{v}}{\partial t} + \vec{v} \cdot \nabla \vec{v}\right) = -\nabla p + \mu \nabla^2 \vec{v} \tag{2}$$

where: ρ – density of blood, $\vec{v}$ -velocity field, p – pressure, μ = co-efficient of viscosity.

In non-dimensional, non-conservative form N-S equations are written as follows:

$$\nabla \cdot \vec{v} = 0$$

$$\frac{\partial \vec{v}}{\partial t} + \vec{v} \cdot \nabla \vec{v} = -\nabla p + \frac{1}{\mathrm{Re}_L} \nabla^2 \vec{v} \qquad (3)$$

In vector form,

$$\frac{\partial \vec{Q}}{\partial t} + \frac{\partial \vec{E}_i}{\partial x} + \frac{\partial \vec{F}_i}{\partial y} = \frac{\partial \vec{E}_v}{\partial x} + \frac{\partial \vec{F}_v}{\partial y} \qquad (4)$$

Where $\vec{Q}, \vec{E}_i, \vec{F}_i, \vec{E}_v, \vec{F}_v$ are the vectors containing the primitive variable, inviscid and viscous fluxes in x, y directions,

$$\vec{Q} = \begin{bmatrix} 0 \\ u \\ v \end{bmatrix}, \vec{E}_i = \begin{bmatrix} u \\ u^2 + p \\ uv \end{bmatrix}, \vec{F}_i = \begin{bmatrix} v \\ vu \\ v^2 + p \end{bmatrix}, \vec{E}_v = \begin{bmatrix} 0 \\ \tau_{xx} \\ \tau_{xy} \end{bmatrix}, \vec{F}_v = \begin{bmatrix} 0 \\ \tau_{yx} \\ \tau_{yy} \end{bmatrix}$$

Shear stresses are expressed as $\tau_{xx} = \frac{2}{\mathrm{Re}_L} u_x$, $\tau_{yy} = \frac{2}{\mathrm{Re}_L} v_y$, $\tau_{xy} = \frac{1}{\mathrm{Re}_L}(u_y + v_x)$, $\tau_{xy} = \tau_{yx}$ (5) Joel. Guerrero,[16].

Mesh was generated in Gambit and the input boundary conditions are

u = 0, v = 0, w = 0, on dilated vessel,
v = v_0 according to inlet pressure and velocity
u = 0, w = 0, on inflow segment

Inlet pressure,

i) p = 12,000 pa = 90.0074 mmHg, (low systolic/high diastolic pressure)
ii) P = 20,000 pa = 150.0123 mmHg, (high systolic pressure)
iii) P = 24,000 pa = 180.0148 mmHg (high systolic pressure)

Inlet velocity,

i) v = –0.4 m/s
ii) v = –0.6 m/s
iii) v = –1.5 m/s ('–' sign shows the flow occurs in the downward direction)

Physical properties of blood taken for analysis are density ρ = 1060 [kg/m^3] and co-efficient of viscosity μ = 0.003 [kg/m-s] (Poiseuille). No slip boundary condition is assumed. The body forces are ignored. Although blood has actually non- Newtonian behavior, in the simulation, it is considered Newtonian because there were no significant differences in the distribution of wall shear stress, Yamaguchi. T[16].

The first step in CFD is to discretise the domain into finite control volumes and secondly integrate each control volume yield a discretised equation at its nodal point. The governing equations are discretised using different scheme such as Central differencing, Upwind differencing, and Hybrid differencing. The discretised equations are iteratively solved by using SIMPLE-Semi-Implicit Method for Pressure Linked Equations. SIMPLE is essentially a guess and correct procedure for the calculation of pressure on the staggered grid arrangement.

Algorithm

1. Guessed velocity components is used to evaluate fluxes per unit mass F.
2. Guessed pressure field is used to solve the momentum equations.
3. Guessed pressure is used to solve pressure correction equation deduced from continuity equation.
4. Guess initial velocity and pressure field is required to start iteration process.
5. The process is iterated until convergence of the velocity and pressure fields.

4. Results and Discussion

The grid was generated (Figure 3) and discretised using 15947 nodes, 693 mixed wall faces, 39 mixed pressure outlet faces, 20 mixed pressure inlet faces, 30764 mixed interior faces and 15570 quadrilateral cells.

Contours of velocity magnitude Figure 4a–4e has shown that the flow is not uniform inside the aorta for various inlet conditions. It may vary according to velocities and the different dilations of aneurysms. Very low velocity and recirculation of flow is visible in the aneurysm region implies the stagnation of blood flow and it leads to blood clot. Over the time this may weaken the vessel wall and may rupture. Figure 5a–5c shows the contours of dynamic pressure, which shows the collision of fluid with the vessel wall. In the entrance of the vessel wall there shows high pressure and it reduces with distance. Figure 6a–6b shows the contours of static pressure and Figure 6c shows the total pressure difference inside

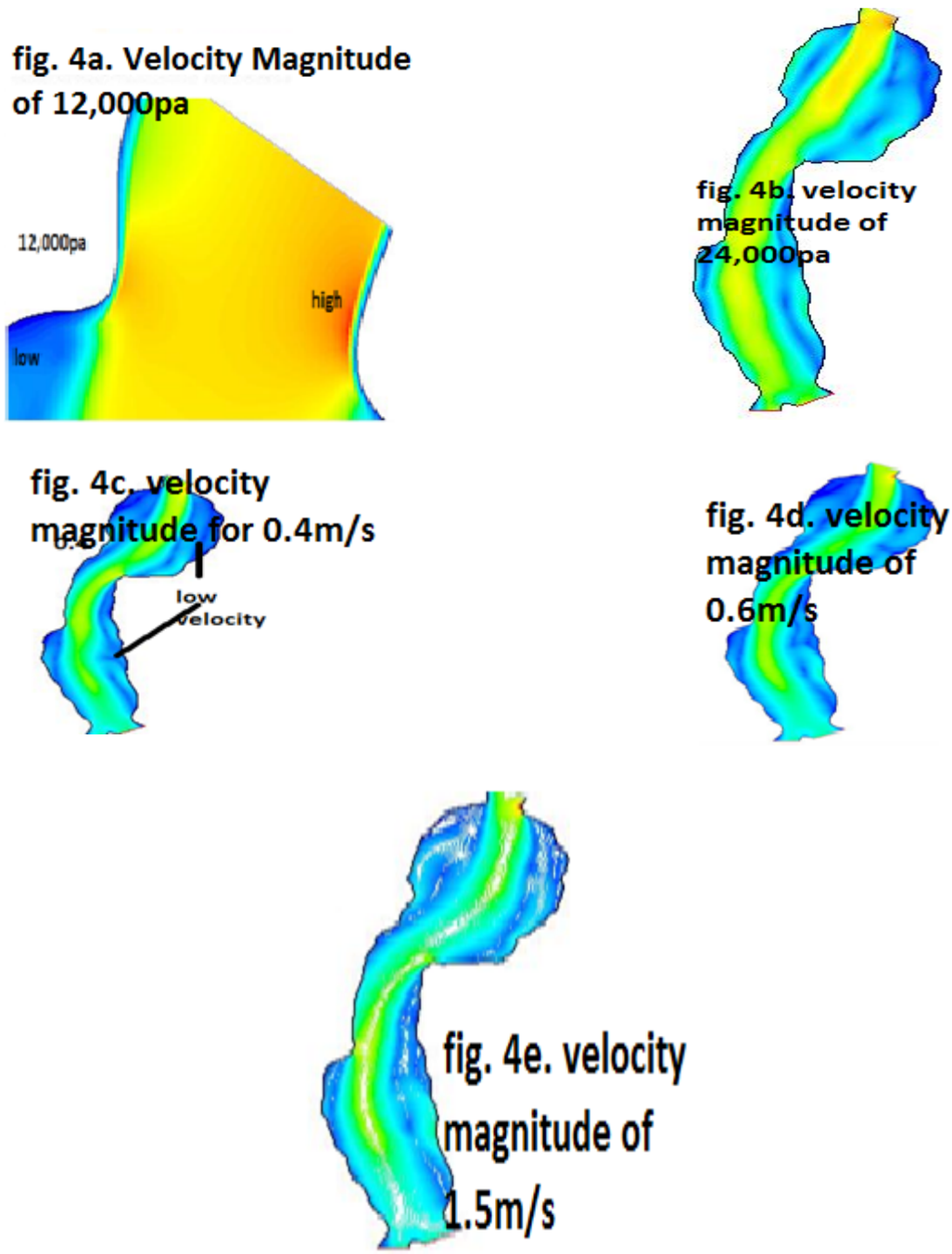

Figure 4. Contours of Velocity Magnitude for different inlets.

the domain. Figure 7a and 7b shows the strain rate and more strain occurs in the neck of the aneurysms than compared with remaining portions. A line that is tangent to velocity vectors is defined as streamlines. Figure 8a–8f shows the streamlines of the velocity vectors coloured by velocity magnitude, dynamic pressure, strain for various inlet pressures and shows the direction of flows inside the aneurysms regions. In the aneurysms region the flow totally varies its path and form a whirlpool. After one or two recirculation it attaches with flow profiles. Figure 8d shows the streamline pattern of strain in the outlet region of bifurcation. Figure 8e and Figure 8f shows the

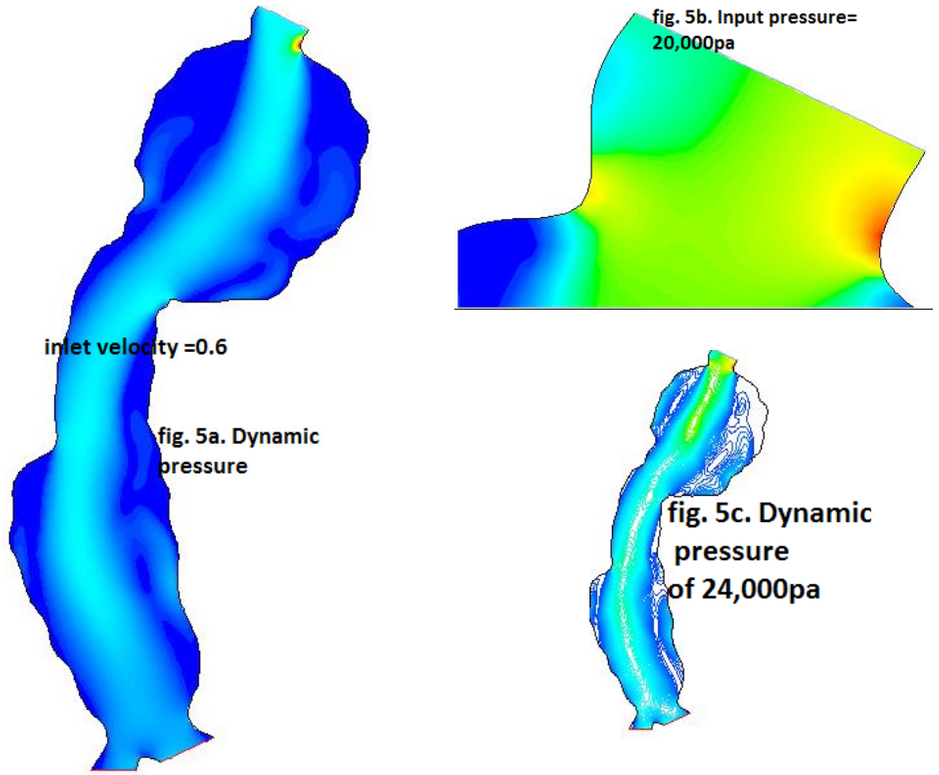

Figure 5. Contours of Dynamic Pressure.

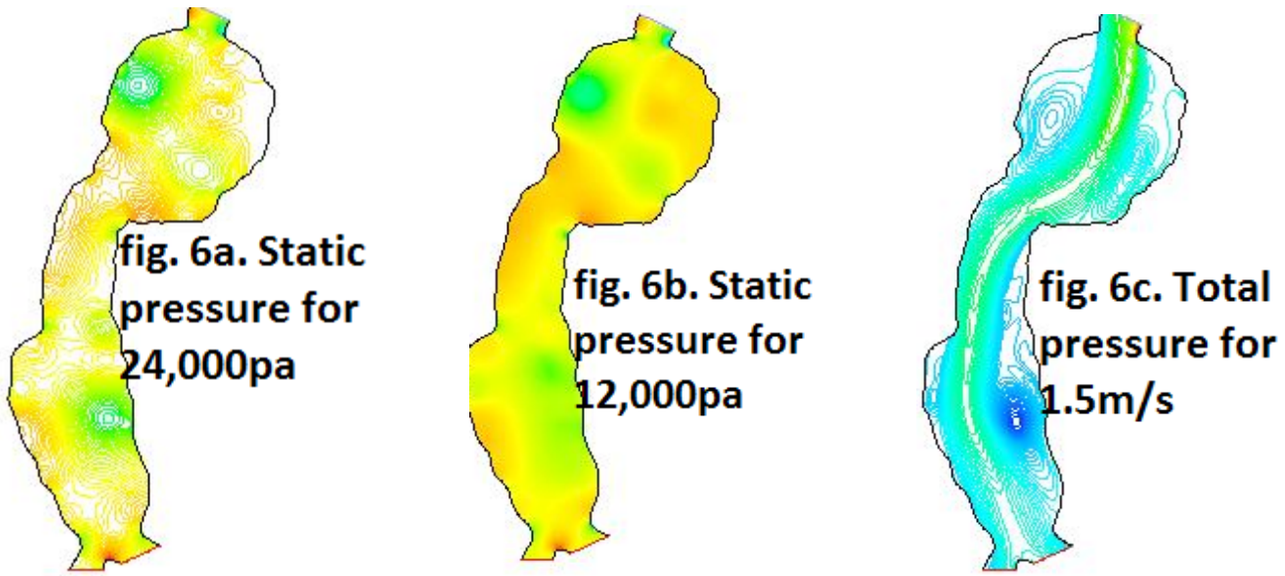

Figure 6. Contours of Static and Total pressure.

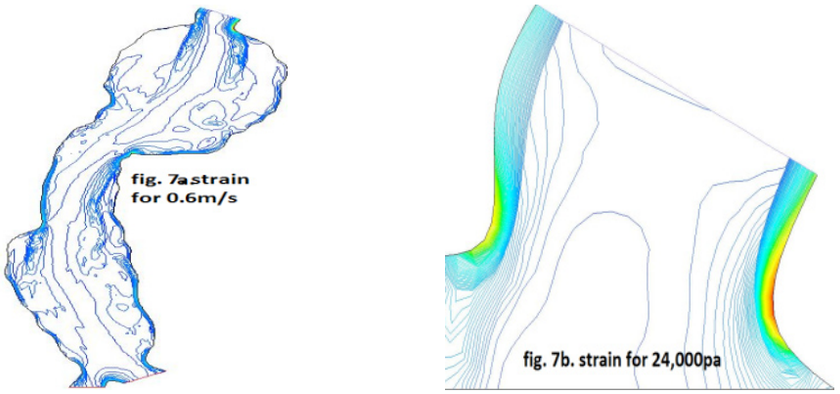

Figure 7. Contours of Strain.

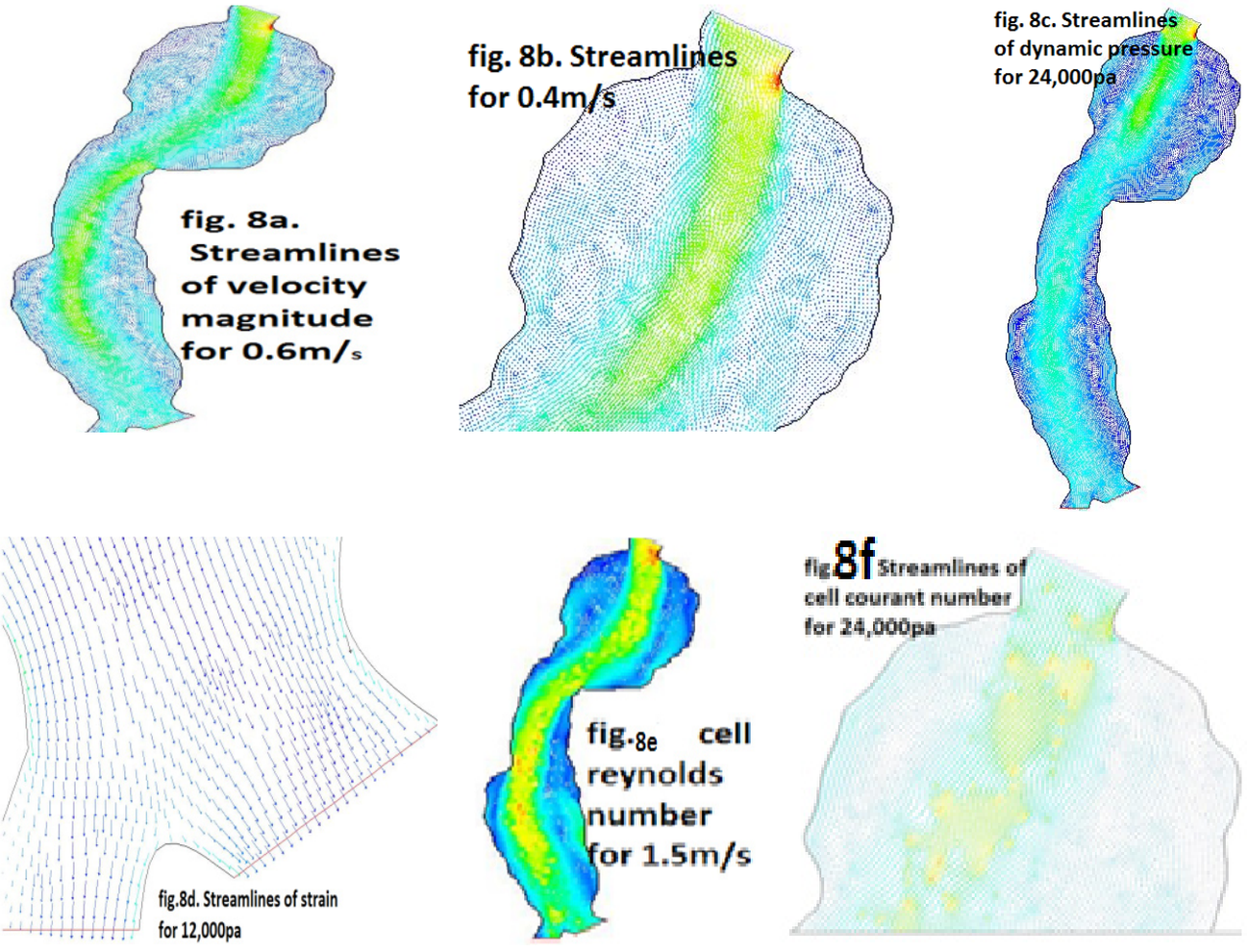

Figure 8. Contours of Streamline patterns.

streamlines of cell reynolds number and cell courant number. Figure 9 shows the x – y plot of dynamic and static pressures, velocity magnitude, wall shear stress, the cell reynolds number and strain for the default interior. Histogram representation of the static and dynamic pressure of the geometry is shown in Figure 10.

Table 1 shows the various ranges (minimum value to maximum value) of hemodynamic factors like dynamic pressure, velocity magnitude, wall shear stress, strain and streamlines of velocity vectors inside the model.

Wall shear stress for the input velocities and pressure has graphically represented in Figure 12.

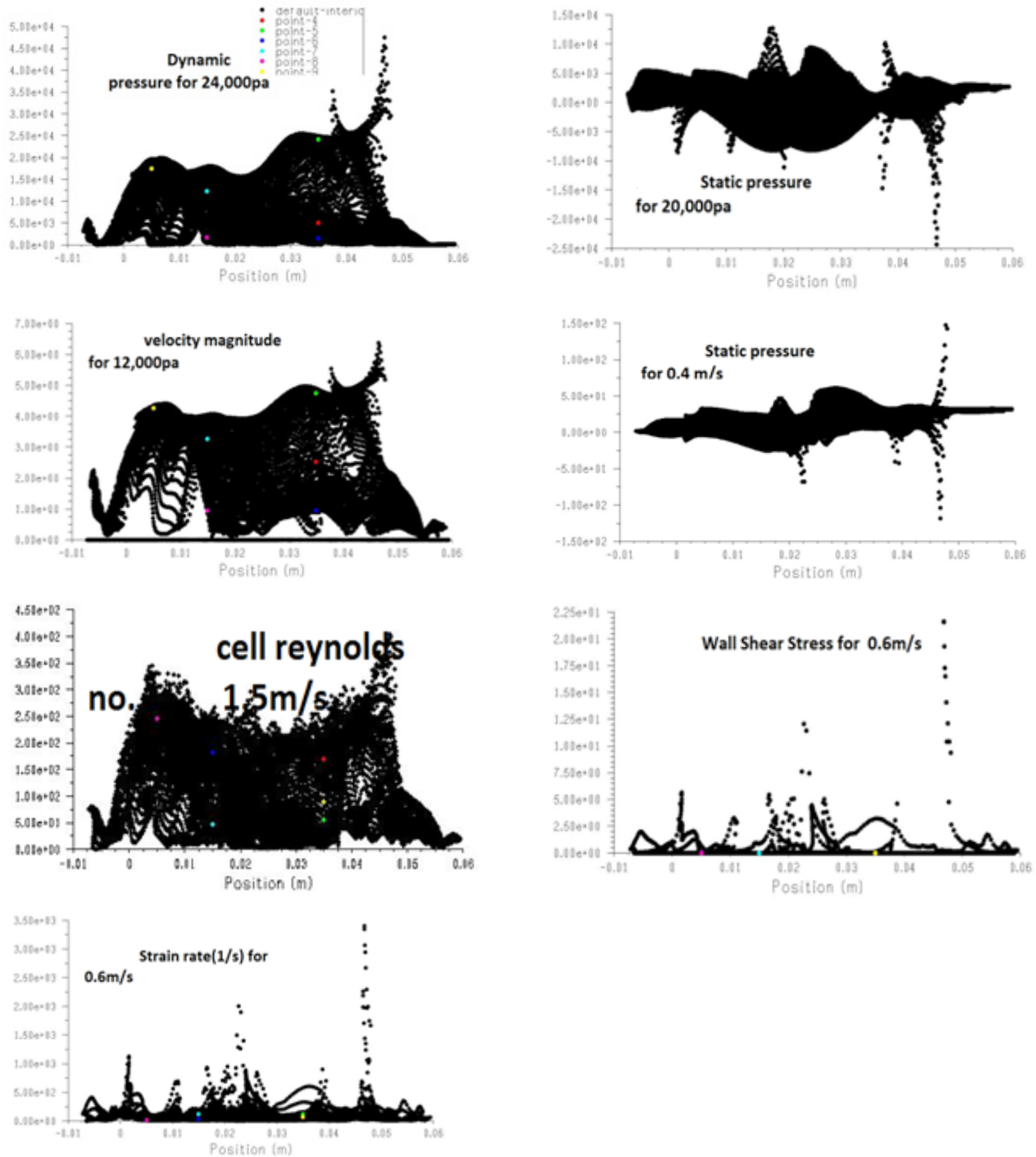

Figure 9. Graphical representation of Pressure, Wall Shear Stress and Strain for different inputs.

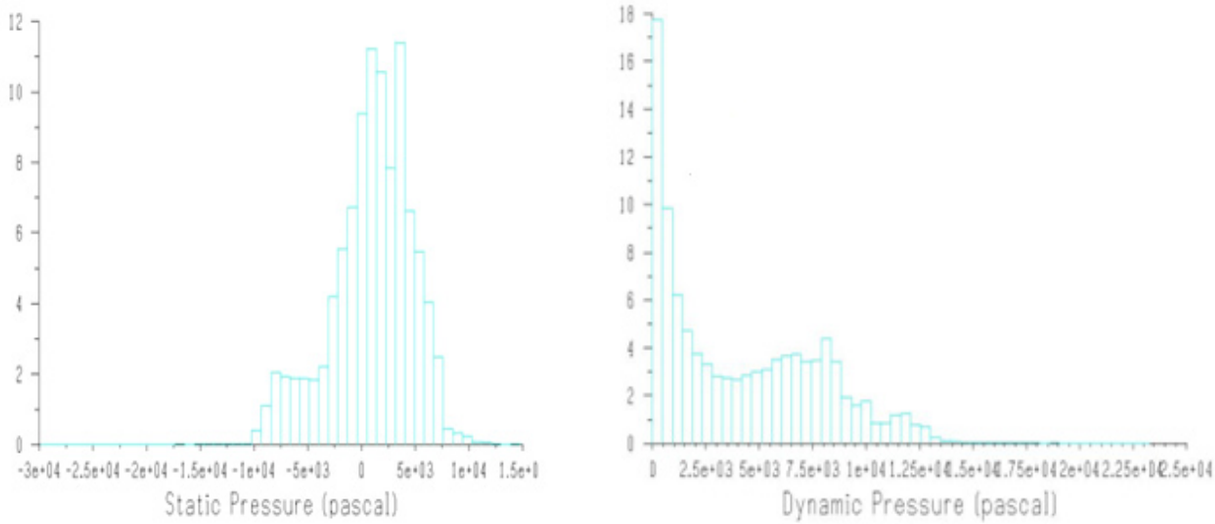

Figure 10. Histogram representation of Static and Dynamic Pressure.

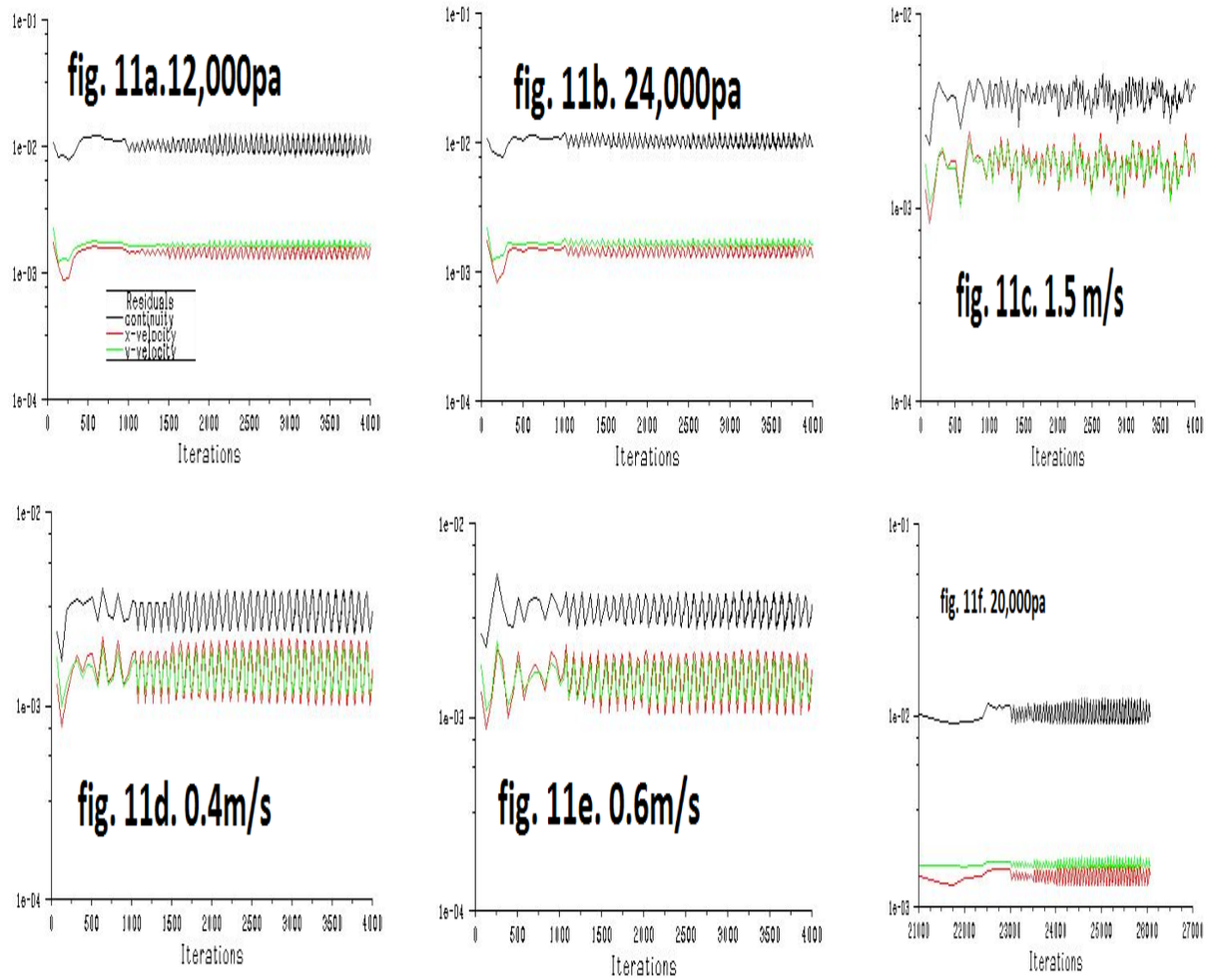

Figure 11. Convergence for different inlet pressures and velocities.

Table 1. Minimum and Maximum values of Hemodynamic factors

Y velocity	0.4	0.6	1.5	4.295226 (12,000 pa)	5.545113 (20000 pa)	6.074367 (24,000 pa)
Dynamic pressure	0.000399 pa–242.2247 pa	0.000668 pa–609.4492 pa	0.01246 pa–4536.721 pa	0.049922 pa–22975.43 pa	0.143176 pa–39869.39 pa	0.6436455 pa–47518.5 pa
Velocity Magnitude	0 m/s–0.655021 m/s	0 m/s–1.02602 m/s	0 m/s–2.732626 m/s	0 m/s–6.372577 m/s	0 m/s–8.38255 m/s	0 m/s–9.14715 m/s
Wall shear stress	0 pa–13.41587 pa	0 pa–21.61005 pa	0 pa–61.14679 pa	0 pa–130.5294 pa	0 pa–171.8988 pa	0 pa–188.3467 pa
Strain	1.5964 (1/s)–2126.14 (1/s)	2.361237 (1/s)–3402.399 1/s)	5.46923 (1/s)–9002.124 (1/s)	13.36139 (1/s)–20365.28 (1/s)	19.52135 (1/s)–26823.12 (1/s)	17.56089 (1/s)–29301.45 1/s)
Streamline vectors	0.0002377 m/s–0.6829402 m/s	0.000355 m/s–1.08569 m/s	0.0021653 m/s–2.937443 m/s	0.006784 m/s–6.622406 m/s	0.014647 m/s–8.730722 m/s	0.023374 m/s–9.533323 m/s

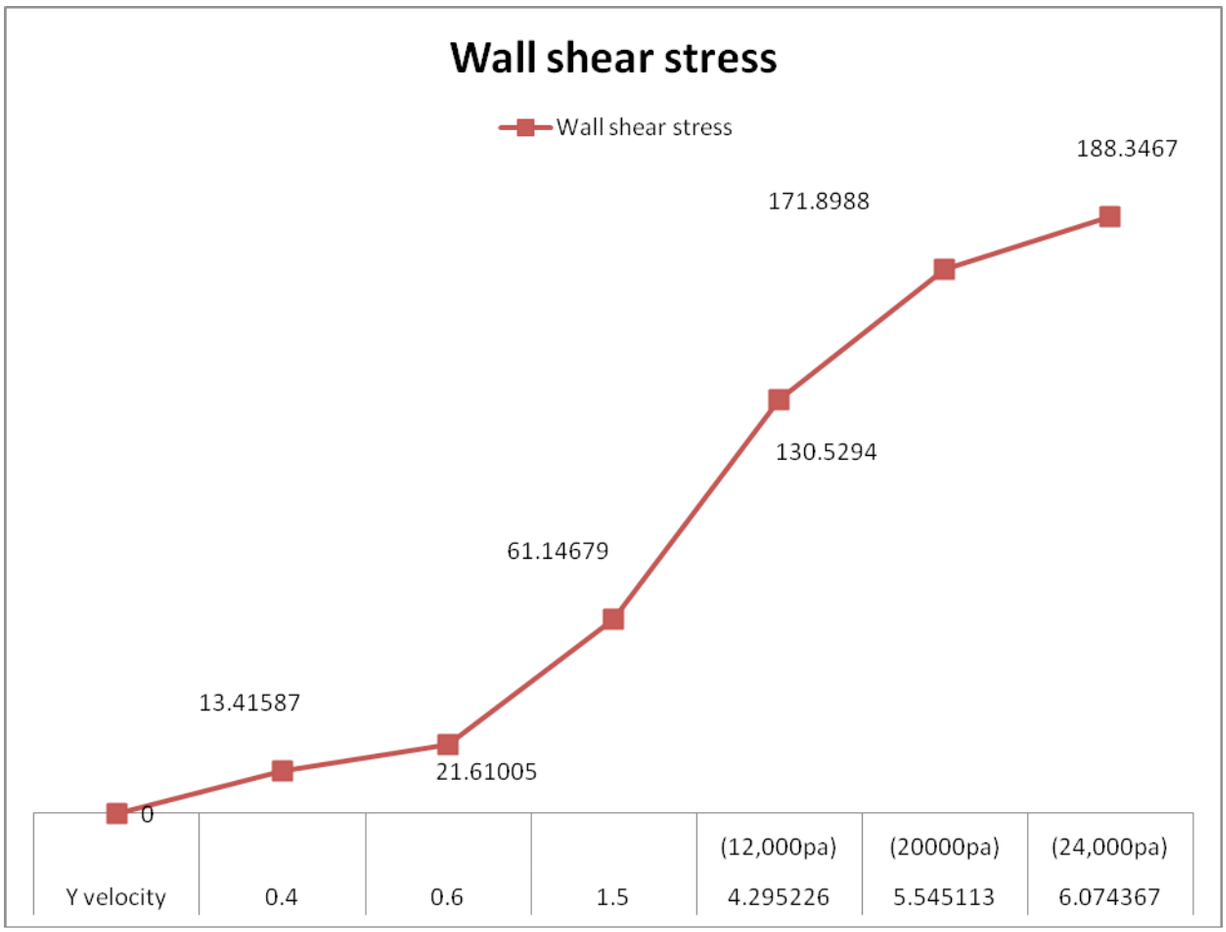

Figure 12. Wall Shear Graph for different inlets.

We see the high WSS for the pressure 24,000 pa which is equal to 6. 074367 m/s i.e. 180mmHg, (High BP, high systolic range).

By considering different points inside the domain shown in Figure 13, we analyze the flow of blood inside the affected aortic aneurysms. Interior points show the various pressures, velocity and strain rate in each point. Compared to point 1, point 2 (near the entrance of the vessel) has high dynamic pressure. By comparing p3 (end portion of 1st aneurysm) and p5 (starting point of second aneurysm) had almost near values compared to the remaining values. We can see a vast difference of values between two neighbouring points p5 and p6 since p6 lie inside the aneurysm region. Table 2, clearly predicts the values of interior points. Point 2 and point 6 have high dynamic pressure and velocity magnitude compared to the remaining points.

Correlation of dynamic pressure between point 2 and point 6 for inlet velocities is 0.99369 < 1 and for inlet pressures is 0.991518 < 1. Similarly between point 4 and point 6 for inlet velocities is 0.974439 < 1 and for pressures 0.941564 < 1. All the values are positive and nearly equal to 1 shows the positive correlation between the points inside the domain. From the graphical representation we shows that the dynamic pressure for p2 is higher than p4 (outlet region) and p6 (inlet of the second aneurysm) and the trendline shows linear equation between points p2 and p6 (y = –1179.7x + 11444).

The Figure 15 shows the 3D histogram representation of complete data set from MIMICS software.

Convergence of governing equations was carried out for 4000 iterations with time step size (s) =10, Number of time steps = 10, Max. Iterations per Time step = 200, Reporting interval = 10 (Table 3). Fig. 11 show the convergence of continuity equation and momentum equations for an unsteady flow (time dependent flow).

In case of non-convergence, some parameters have to be tuned adequately. For explicit solvers the 'cfl' no. and for implicit solvers the under relaxation factors can be changed.

Table 2. Hemodynamic values of 6 interior points

Y Vel. Positions		–0.4	–0.6	–1.5	–4.295226 (12,000 pa)	–5.545113 (20000 pa)	–6.074367 (24,000 pa)
	D P	61.808	153.438	835.85	3384.42	5503.04	5067.6
P1	V M	0.3415	0.4463	1.2558	2.5249	3.2207	3.0879
	STR	30.3088	32.6718	83.855	365.13	400.231	445.407
	DP	16.7945	24.73	55.501	11981	20463.8	24180.8
P2	VM	0.175943	0.200644	0.3068	4.7543	6.21344	6.75421
	STR	70.9192	116.675	299.31	85.6307	86.246	89.0467
	DP	50.5439	127.449	537.33	479.14	620.228	1516.52
P3	VM	0.308799	0.446388	1.0067	0.95004	1.08043	1.6905
	STR	14.9417	26.5113	91.731	327.725	422.578	460.874
	DP	12.4651	23.6	48.19	5651.65	8989.9	12230.1
P4	VM	0.152864	0.058022	0.3006	3.26465	4.11784	4.80276
	STR	48.6689	81.3595	158.22	128.099	189.56	248.541
	DP	53.51	143.065	1163.4	497.896	1451.87	1749.28
P5	VM	0.31769	0.557552	1.4816	0.94422	1.65488	1.8066
	STR	18.8787	29.2567	14.936	1308.42	1002.67	857.457
	DP	5.22543	16.3618	126.87	9621.64	16059.2	17489.2
P6	VM	0.09896	0.118638	0.4873	4.26059	5.50451	5.74441
	STR	52.1576	79.515	174.91	212.871	198.54	120.39

Where DP = dynamic pressure, VM = velocity magnitude STR = strain

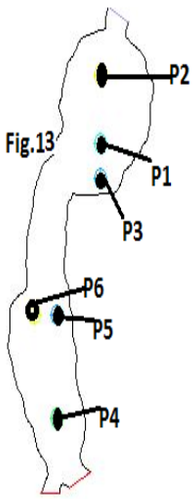

Figure 13. Six interior points for analysis

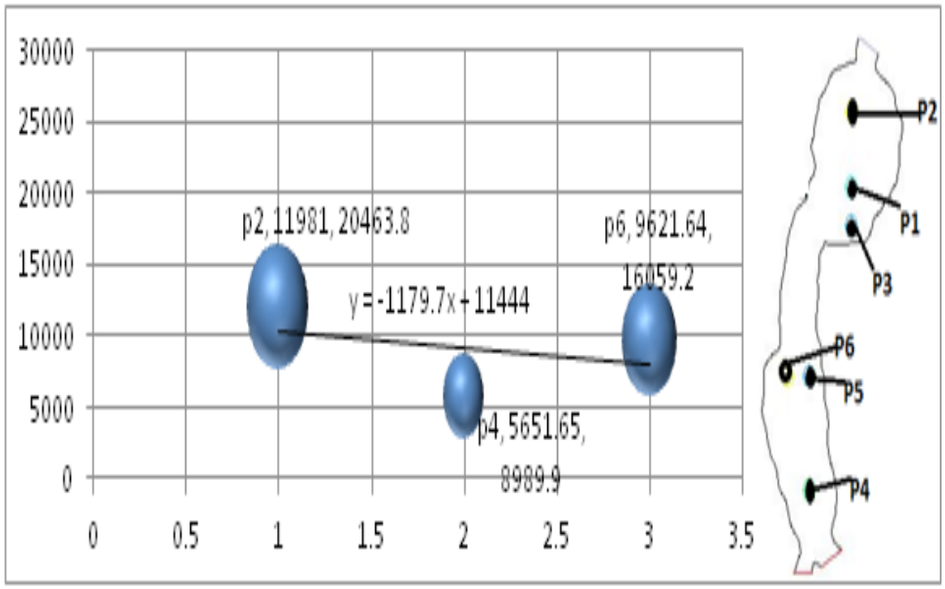

Figure 14. Line of Regression between the points.

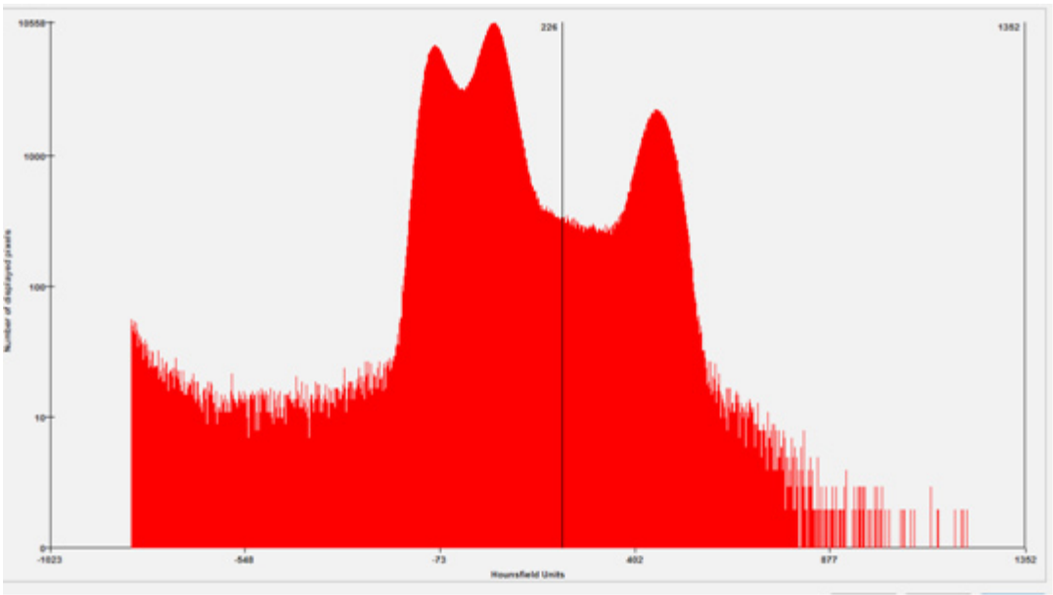

Figure 15. 3D Histogram representation of cropped image from MIMICS Software.

Table 3. 4000 iterations in 200 seconds

Y velocity	−0.4	−0.6	−1.5	−4.295226 (12,000 pa)	−5.545113 (20000 pa)	−6.074367 (24,000 pa)
Continuity	0.003038	0.0038206	0.0041506	0.011503	0.0096316	0.0093568
X	0.001539	0.0017557	0.0016258	0.0015657	0.0014239	0.0013089
y	0.001388	0.0015847	0.0015256	0.0017209	0.0016316	0.0016153

5. Conclusion

The main cause of aortic aneurysms is atherosclerosis and high blood pressure. Most aortic aneurysms have no symptoms. They are diagnosed with a chest X-ray or computerized tomography (CT) scan and Magnetic resonance imaging (MRI). This kind of the CFD study of flow analysis is designed to prove a concept under assumptions which may not be true in reality. Flow analysis shows that flow model is not similar for all aneurysms. Flow characteristics are highly dependent on the geometry of the vessels and aneurysms. The low blood velocity near the vessel wall shows blood moves slowly where it needs to go. The decreased rate of flow can lead to deoxygenating, as less blood will be reaching certain areas, and therefore those areas will be starved of oxygen. The results show due to high blood pressure there is vigorous motion of blood inside the aorta. Already the vessel wall is very thin due to aneurysms may easily tear and blood may ooze out and this leads to blood clot. Results show that the pressure is very high in the aneurysm region (p6, p2) than in the remaining regions. Similarly velocity profiles may vary at different positions. So the risk of rupture is higher in the patient with high blood pressure having aortic aneurysms than with other normal aortic aneurysms persons. The medical treatment includes control of blood pressure and heart rate and next is the replacement of the aneurysm portion of aorta with an artificial graft if needed. After surgery further medication is required and the patient should practice the following: 1. Quit smoking 2. Regular exercise 3. Reduce or maintain weight 4. Reduce intake of cholesterol 5. Maintain blood pressure 6. Regular checkup.

6. References

1. Taylor CA, Hughes TJR, Zarins CK. Finite element modeling of blood flow in arteries, Comput Meth Appl Mech Eng. 1998; 158(1):155–96.
2. Shipkowitz T, Rodgers VGJ, Frazin LJ, Chandran KB. Numerical study on the effect of secondary flow in the human aorta on local shear stresses in abdominal aortic branches. J Biomech. 2000; 33(6):717–28.
3. Yamaguchi T. Computational mechanical model studies in the cardiovascular system. Clinical Application of Computational Mechanics to the Cardiovascular system. Springer; 2000. p. 3–18.
4. Lee D, Chen JY. Numerical simulation of steady flow fields in a model of abdominal aorta with it peripheral branches. J Biomech. 2002; 35:1115–22.
5. Formaggia L, Gerbean JF, Nobile F, Quarteroni A. On the coupling of 3D and 1D NS equations for flow problems in compliant vessels. Comput Meth Appl Mech Eng. 2001; 191:561–82.
6. Formaggia L, Nobile F, Quarteroni A, Veneziani A. Multiscale modeling of the circulatory system. Computing and Visualisation Sci. 1999; 2:75–83.
7. Malek AM, Izumo S. Mechanism of endothelial cell shape change and cytoskeletal remodeling in response to fluid shear stress. Journal of Cell Science. 1996; 109:713–26.
8. Wille SO. Finite element simulations of the pulsatile blood flow patterns in arterial abnormalities. Finite Elemens In Biomechanics. 1982. p. 39–60.
9. Perktold K. On the paths of fluid particles in an axisymmetrical aneurysm. J Biomech. 1987; 20(3):311–7.
10. Kumar RBV, Naidu KB. Hemodynamics in Aneurysm. Computers and Biomedical Research. 1996; 29:119–39.
11. Perktold, Kenner, Hilbert, Sport, Florian. Numerical blood flow analysis in arterial bifurcation with a saccular aneurysm. Basic Res Cardiology. 1988; 83:24–31.
12. Taylor T, Yamaguchi T. Three dimensional simulation of blood flow in an abdominal aortic aneurysm – steady and unsteady flow cases, 1994. J Biomech Eng. 1994; 116:89–97.
13. Liang-Der J, Mawad ME. Growth rate and rupture rate of unruptured intracranial aneurysms a population approach. Biomedical Engineering OnLine. 2009; 8(11).
14. Roy D, Kauffmann C, Delorme S. A Literature Review of the Numerical Analysis of Abdominal Aortic Aneurysms Treated with Endovascular stent Grafts. Computational and Mathematical Methods in Medicine. 2012; 2012. 1–16. Article ID 820389.
15. McDonald DA. Blood Flow in Arteries, Camelot, Baldwin Park, CA 1974.
16. Guerrero J. Numerical Simulation of the Unsteady Aerodynamics of Flapping Flight. [Ph.D thesis]. Chapter 3, 2009; University of Genoa. p. 34–51.